Chapter 18
A Study of Phase Equilibria in the Al–Pd–Co System at 700 °C

I. Černičková, R. Čička, P. Švec, D. Janičkovič, P. Priputen, and J. Janovec

Abstract $Al_{68}Pd_{14.6}Co_{17.4}$, $Al_{69.8}Pd_{13.8}Co_{16.4}$, $Al_{72}Pd_{12.8}Co_{15.2}$, $Al_{73.8}Pd_{11.9}Co_{14.3}$, and $Al_{76}Pd_{11}Co_{13}$ alloys annealed at 700 °C for 2000 h were studied. In the investigation, scanning electron microscopy including energy dispersive X-ray spectroscopy and electron backscatter diffraction, X-ray diffraction, and transmission electron microscopy were used. Altogether five near-equilibrium phases (β, U, Al_5Co_2, ε, Al_9Co_2) were identified. Transitions between β, U, and ε phases were also determined dependent on the alloy bulk metal composition. The experimental results were used to propose the partial isothermal section of the Al–Pd–Co phase diagram at 700 °C. The maximum solubilities at 700 °C of Pd in Al_9Co_2 and Al_5Co_2 were determined as 1.7 and 2.69 at.%, respectively.

18.1 Introduction

Structurally complex phases consisting of large cluster-base unit cells are attributed to complex metallic alloys (CMA) inclusive of ternary Al-base CMAs [1–5]. In the Al–Pd–Co alloys, more structurally complex phases were observed [6–11], e.g., the ternary monoclinic U-phase or orthorhombic phases of the ε-family. The latter phases can be classified as either binary phases alloyed with the third element (ε_6 and ε_{28}) or ternary phases (ε_{22} and ε_{34}) [12]. Yurechko et al. [6, 7, 9, 11] studied phase equilibria in the Al–Pd–Co system and published isothermal sections of the related phase diagram at 1050, 1000, 940, and 790 °C.

In the present work, five ternary alloys ($Al_{68}Pd_{14.6}Co_{17.4}$, $Al_{69.8}Pd_{13.8}Co_{16.4}$, $Al_{72}Pd_{12.8}Co_{15.2}$, $Al_{73.8}Pd_{11.9}Co_{14.3}$, and $Al_{76}Pd_{11}Co_{13}$) were long-term annealed at 700 °C and the near-equilibrium phases formed were characterized. The exper-

I. Černičková (✉) · R. Čička · P. Švec · P. Priputen · J. Janovec
Faculty of Materials Science and Technology in Trnava, Slovak University of Technology in Bratislava, Paulínska 16, 917 24 Trnava, Slovak Republic
e-mail: ivona.cernickova@stuba.sk

P. Švec · D. Janičkovič
Institute of Physics, Slovak Academy of Sciences, Dúbravská 9, 845 11 Bratislava, Slovak Republic

S. Schmid et al. (eds.), *Aperiodic Crystals*, DOI 10.1007/978-94-007-6431-6_18,
© Springer Science+Business Media Dordrecht 2013

iment was done with the intention to propose a partial isothermal section of the Al–Pd–Co phase diagram at 700 °C still missing in the literature.

18.2 Experimental Procedures

The investigated alloys were prepared by arc melting of pure components under argon atmosphere. After casting, the samples were annealed at 700 °C for 2000 h and rapidly cooled in water to fix their high-temperature microstructure.

In the investigation, scanning electron microscopy (SEM) including energy dispersive X-ray spectroscopy (EDX) and electron backscatter diffraction (EBSD), X-ray diffraction (XRD), and transmission electron microscopy (TEM) were used. For XRD a Philips PW 1830 diffractometer with Bragg–Brentano geometry was selected using iron filtered $Co_{K\alpha 1}$ radiation, scattering angle 2θ ranged between 5 and 70°, step size was 0.02°, and exposure time was 10 s per step. For SEM a JEOL JSM-7600F microscope was used equipped with an EDX spectrometer X-max working with INCA software and an EBSD Nordlys detector working with FLAMENCO software. At least 10 measurements per microstructure constituent were performed to determine their metal compositions. To calculate volume fractions of microstructure constituents an ImageJ software was used. The identification of phase by selected-area electron diffraction (SAED) was performed in a JEOL 2000FX microscope operating at 200 kV.

18.3 Results

The results of the characterization of near-equilibrium phases present in particular alloys are summarized in Table 18.1. Each of the observed microstructure constituents was found to consist of a single phase. For instance, the single-phase constituents observed in the $Al_{76}Pd_{11}Co_{13}$ alloy (Fig. 18.1) were identified as ε and Al_9Co_2 (Fig. 18.2). Altogether five phases were found in the investigated alloys. Monoclinic U, cubic β, orthorhombic ε, and monoclinic Al_9Co_2 were identified by XRD because their volume fractions were detectable for this technique (compare Table 18.1 and Fig. 18.2). These phases were also identified by SAED/TEM as documented in Fig. 18.3 for β. For the identification of hexagonal Al_5Co_2 appearing in extremely small amounts in $Al_{68}Pd_{14.6}Co_{17.4}$ and $Al_{69.8}Pd_{13.8}Co_{16.4}$ alloys, the EBSD/SEM technique was used (Fig. 18.4). Metal compositions and volume fractions of the identified near-equilibrium phases are also given in Table 18.1.

18.4 Discussion

The experiments were done with the aim to find correlations between the microstructure constituents (SEM), the identified near-equilibrium phases (XRD,

Table 18.1 Overview of experimental results. Observed microstructure constituents, identified phases, and metal compositions and volume fractions of the phases are given in respective columns for all the investigated alloys. Experimental techniques used are related to the obtained results (see two bottom rows)

Microstructure constituent	Phase	Atomic content in %			Volume fraction in %
		Al	Co	Pd	
$Al_{68}Pd_{14.6}Co_{17.4}$					
grey	U	68.85 ± 0.12	16.14 ± 0.12	15.01 ± 0.09	92.8
white	β	57.61 ± 0.26	8.13 ± 0.13	34.26 ± 0.18	6.6
dark	Al_5Co_2	72.52 ± 0.1	25.42 ± 0.11	2.06 ± 0.06	0.6
$Al_{69.8}Pd_{13.8}Co_{16.4}$					
grey	U	69.09 ± 0.16	15.13 ± 0.14	15.78 ± 0.11	99.4
dark	Al_5Co_2	72.47 ± 0.19	24.84 ± 0.19	2.69 ± 0.05	0.6
$Al_{72}Pd_{12.8}Co_{15.2}$					
darker grey	ε	72.78 ± 0.81	14.60 ± 0.93	12.62 ± 0.49	87.5
lighter grey	U	69.92 ± 0.21	15.47 ± 0.64	14.62 ± 0.52	12.5
$Al_{73.8}Pd_{11.9}Co_{14.3}$					
grey	ε	73.0 ± 0.14	14.1 ± 0.12	12.9 ± 0.13	100
$Al_{76}Pd_{11}Co_{13}$					
grey	ε	74.2 ± 0.21	12.7 ± 0.19	14.1 ± 0.08	71.5
dark	Al_9Co_2	81.8 ± 0.05	16.5 ± 0.05	1.7 ± 0.03	28.5
Experimental technique used					
SEM	XRD, SAED/TEM EBSD/SEM	EDX/SEM			SEM

SAED/TEM, EBSD/SEM), as well as metal compositions (EDX/SEM) and volume fraction (SEM) of the identified phases. Bulk metal compositions of the investigated alloys were selected with the intention to hold the Pd/Co-ratio constant. Thus, an increase in the Al bulk content was accompanied by a decrease in both Pd- and Co-bulk contents. As follows from Fig. 18.5, there is a correlation between the bulk Al content and the occurrence of dominant phases in the investigated alloys. The increase in the Al bulk content from 68 to 76 at.% evoked $\beta + \mathrm{U} \rightarrow \mathrm{U} \rightarrow \mathrm{U} + \varepsilon \rightarrow \varepsilon$ phase transitions. This shows that Al stabilizes mainly ε and Pd + Co stabilize mainly β in the investigated alloys. Moreover, the Al contents in both U and ε were found to increase slightly with increasing the bulk Al content in agreement with [6–8].

The partial isothermal section of the Al–Pd–Co phase diagram (in the next text shortly "diagram") at 700 °C (Fig. 18.6) was proposed with respect to both own experimental results and the diagram published by Yurechko for 790 °C [7]. Positions and sizes of single-phase ε and U areas were modified only slightly. The double-phase $\varepsilon + \mathrm{U}$ area became wider. The positions of $\varepsilon + Al_9Co_2$ and $\mathrm{U} + \beta + Al_5Co_2$

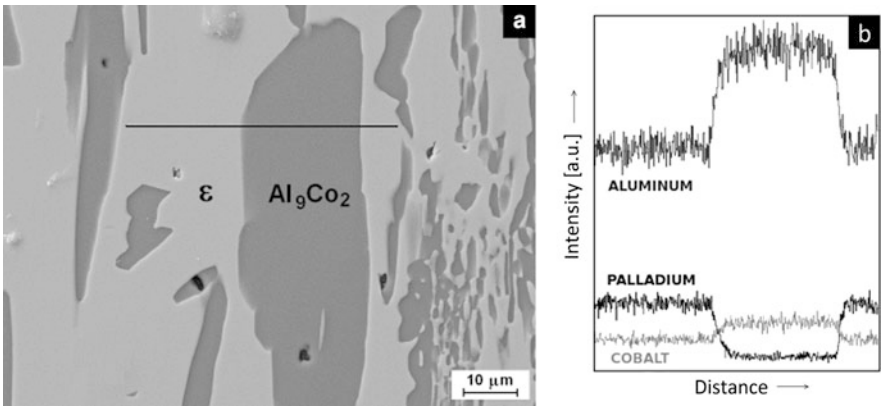

Fig. 18.1 SEM micrograph showing single-phase microstructure constituents (the phases were determined by XRD) in $Al_{76}Pd_{11}Co_{13}$ alloy (**a**) and compositional changes along the indicated line determined by EDX (**b**)

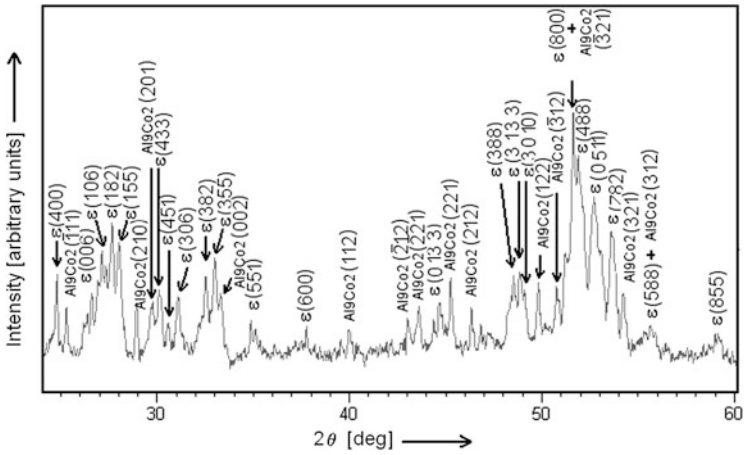

Fig. 18.2 Powder X-ray diffraction pattern corresponding to $Al_{76}Pd_{11}Co_{13}$ alloy

areas are extended towards the higher Pd contents. Dashed lines were used when experimental results were not available. The F-phase was not found experimentally after long-term annealing at 700 °C. It confirms the trend reported in [7, 8] that F disappears gradually with decreasing temperature. This happens probably between 790 and 700 °C. Several binary Al–Co and Al–Pd phases exhibit extensions into the ternary compositional area. At 700 °C, the maximum solubilities of Pd in Al_9Co_2 and Al_5Co_2 were determined as 1.7 and 2.69 at.%, respectively. Congruent AlCo and AlPd phases of the CsCl-type were found to form continuous set of β-Al (Pd, Co) solid solutions [7–9].

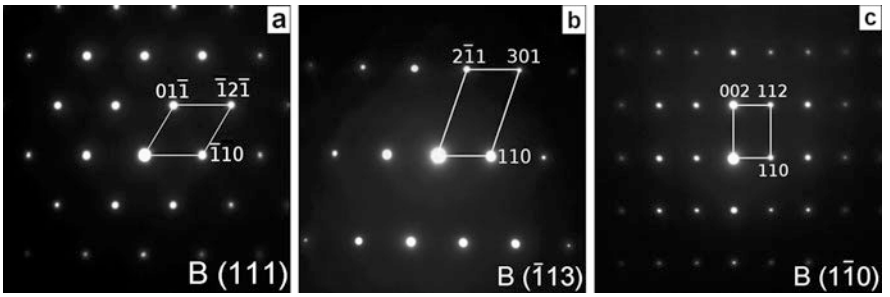

Fig. 18.3 SAED/TEM patterns of β in $Al_{68}Pd_{14.6}Co_{17.4}$ alloy with three different zone axes

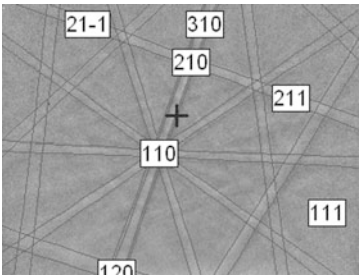

Fig. 18.4 EBSD/SEM pattern of Al_5Co_2 in $Al_{68}Pd_{14.6}Co_{17.4}$ alloy

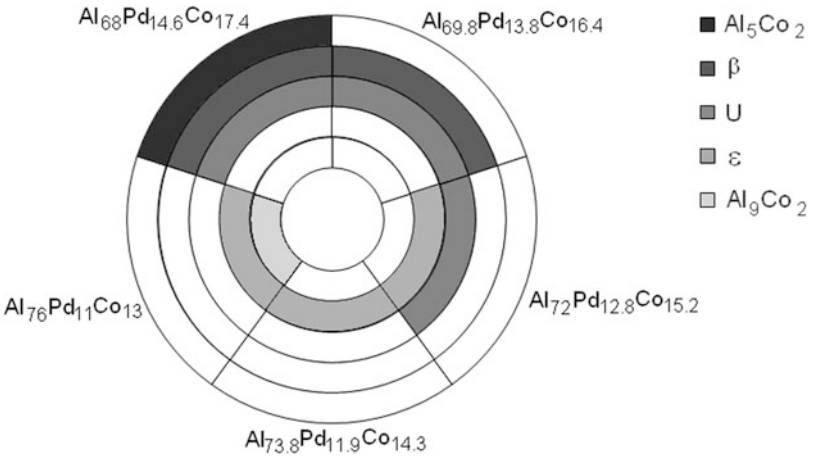

Fig. 18.5 Schematic diagram showing transitions in phase occurrence in dependence on alloy bulk composition

18.5 Conclusions

In the investigated $Al_{68}Pd_{14.6}Co_{17.4}$, $Al_{69.8}Pd_{13.8}Co_{16.4}$, $Al_{72}Pd_{12.8}Co_{15.2}$, $Al_{73.8}Pd_{11.9}Co_{14.3}$, and $Al_{76}Pd_{11}Co_{13}$ complex metallic alloys, altogether five near-equilibrium phases (β, U, Al_5Co_2, ε, Al_9Co_2) were identified after annealing at

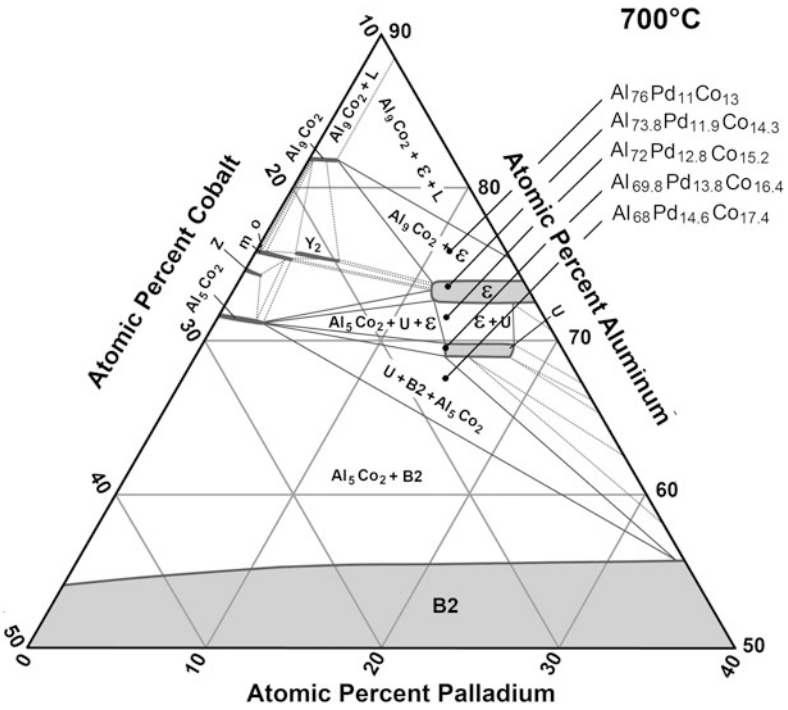

Fig. 18.6 Partial isothermal section of Al–Pd–Co phase diagram proposed for 700 °C with respect to experimental results. In the diagram the symbol B2 is used for β-phase

700 °C for 2000 h. The microstructure constituents, their metal compositions, and volume fraction were assigned to the near-equilibrium phases identified. The increase in the bulk Al content from 68 to 76 at.% was found to evoke $\beta + \mathrm{U} \rightarrow \mathrm{U} \rightarrow \mathrm{U} + \varepsilon \rightarrow \varepsilon$ phase transitions. The partial isothermal section of the Al–Pd–Co phase diagram at 700 °C was proposed based on the experimental results. The maximum solubilities at 700 °C of Pd in Al_9Co_2 and Al_5Co_2 were determined as 1.7 and 2.69 at.%, respectively.

Acknowledgements The authors wish to thank to the European Regional Development Fund (ERDF) for financial support of the project ITMS:26220120014 "Center for development and application of advanced diagnostic methods in processing of metallic and non-metallic materials" funded within the Research & Development Operational Programme, to the Slovak Academy of Sciences for the support in the frame of the "Center of Excellence for functional multiphase materials" (FUN-MAT), to the Slovak Research and Development Agency (APVV) for the financial support under the contract APVV-0076-11, as well as to the Grant Agency of the Ministry of Education, Science, Research, and Sport of the Slovak Republic and the Slovak Academy of Sciences (VEGA) for the financial support under the contracts 1/0143/12, 2/0111/11, and 1/0339/11.

References

1. Wang N, Fung K, Kuo KH (1988) Symmetry study of the Mn–Si–Al octagonal quasicrystal by convergent beam electron diffraction. Appl Phys Lett 52:2120–2121
2. Beeli C, Nissen HU, Robadey J (1991) Stable Al–Mn–Pd quasi-crystals. Philos Mag Lett 63:87–95
3. Dubois JM (2001) Quasicrystals J Phys Condens Matter 13:7753–7762
4. Okabe T, Furihata JI, Morishita K, Fujimori H (1992) Decagonal phase and pseudo-decagonal phase in the Al–Cu–Cr system. Philos Mag Lett 66:259–264
5. Mihalkovič M, Zhu WJ, Henley CL, Phillips R (1996) Icosahedral quasicrystal decoration models, II: optimization under realistic Al–Mn potential. Phys Rev B 53:9022–9044
6. Yurechko M, Grushko B (2000) A study of the Al–Pd–Co alloy system. Mater Sci Eng A 294:139–142
7. Yurechko M, Grushko B, Velikanova T, Urban K (2002) Isothermal sections of the Al–Pd–Co alloy system for 50–100 at% Al. J Alloys Compd 337:172–181
8. Raghavan V (2008) Al–Pd–Co. J Phase Equilib 29:54–56
9. Yurechko M, Fattaha A, Velikanova T, Grushko B (2001) A contribution to the Al–Pd phase diagram. J Alloys Compd 329:173–181
10. Matsuo Y, Hiraga K (1994) The structure of Al3Pd—close relationship to decagonal quasi-crystals. Philos Mag Lett 70:155–161
11. Yurechko M, Grushko B, Velikanova T, Urban K (2004) A comparative study of the Al–Co–Pd and Al–Co–Ni alloy system. J Alloys Compd 367:20–24
12. Frigan B, Santana A, Engel M, Schopf D, Trebin H-R, Mihalkovič M (2011) Low-temperature structure of ξ-Al–Pd–Mn optimized by ab initio methods. Phys Rev B 84:184203